

Stimulation of CO₂ solubility in reversible ionic liquids activated by novel 1-(2-aminoethyl) piperazine and bis (3-aminopropyl) amine

Sweta C Balchandani ^{a,b}, Bishnupada Mandal ^{a,*}, Swapnil Dharaskar ^b

^a Department of Chemical Engineering, Indian Institute of Technology, Guwahati 781039, India

^b CO₂ Research Group, Department of Chemical Engineering, Pandit Deendayal Petroleum University, Gandhinagar 382007, India



ARTICLE INFO

Keywords:

VLE of CO₂

TESA

AEP

APA

Modified Kent-Eisenberg

Reversible ionic liquids

ABSTRACT

The quest of energy efficient post combustion CO₂ capture through an integrated process approach leads to the development of various novel solvents which can yield the necessary outputs. In line with this, the current work explores the experimental and simulation analysis of vapor liquid equilibrium of CO₂ in novel aqueous 3-aminopropyl triethoxysilane (TESA) solvent blends enhanced by amine activators. Specific amine activators, viz. 1-(2-aminoethyl) piperazine (AEP) and bis (3-aminopropyl) amine (APA) were considered. The experiments were carried out over the temperature range of (303.2–323.2) K and pressure of (4–350) kPa. In order to realize the effect of activator, AEP/ APA concentration was gradually increased from 0.5 to 1.0 mol/kg with a total solvent concentration of ≈3 mol/kg. Along with this, qualitative ¹³C NMR and FTIR analysis were also performed to assess the proposed reaction scheme. The experimental vapour liquid equilibrium data (VLE) were correlated by modified Kent-Eisenberg equilibrium model considering gas phase non-ideality as well as non-rigorous statistical non-linear model. The equilibrium constants associated to deprotonation of protonated TESA, AEP and APA as well as carbamate formation reactions of these amines with CO₂ are function of solvent concentration, temperature and CO₂ partial pressure. These are regressed to fit the experimental VLE data. The modified KE model is further prolonged to estimate the concentration profiles of various molecular and ionic species involved in the reactive system.

1. Introduction

One of the major thrust areas for the energy sector is the control of emissions as well as effective capture of CO₂-an important greenhouse gas. The absorption of CO₂ majorly is being done either by post-combustion or pre-combustion processes. Recently, modern technologies such as hydrate based gas separation have also been proposed for CO₂ capture in pre-combustion processes [1]. Whereas for post combustion CO₂ capture, there are a variety of applicable processes such as absorption, adsorption, membrane separations, cryogenic separation, etc. However, majorly absorption based process has always held upper hand in comparison to others due to ease of retrofitting in the existing plants.

Generally, while CO₂ is being captured, the achieved efficiency is lost almost at an extent of 10% due to energy demand of the process itself therefore establishing the overall process carbon positive. Further, the overall cost of carbon capture systems is highly dictated by the configurations and alignments of absorption and desorption towers, number

and type (single pressure or bi-pressure) of towers involved, the counter or co-current flow of associated streams, number and type of intercoolers or boilers required, etc. If the configuration selected is optimized, then it can result in cost gain by 2–5 % as well as energy demand reduction by 4–7 % which can drastically reduce the overall separation cost [2]. A delta increment in the efficiency of CCS process is also valued in the industries [3]. Hence, the efficiency of carbon capture and sequestration (CCS) systems and further having a pure CO₂ stream for storage or utilization depends on diverse factors. This can be categorized as multi-objective problem with constraints. Major constraints involved are liquid to gas flow rate, heat supplied, compression power, volume of lean solvent for stripper and reboiler, amount of steam required for reboiler duty, etc. [4]. Therefore, for energy saving and cost reduction, optimum and efficient solvent selection is one of the key criteria, which is able to reduce the operational costs related to regeneration and pumping of solvents [5].

CO₂ has been absorbed using many solvents primarily amines, blended amines or other physical solvents [6,7]. Traditionally applied

* Corresponding author.

E-mail address: bpmandal@iitg.ac.in (B. Mandal).

Table 1

Specifications of the Chemicals used in the Present Work.

Chemical Name	Chemical Structure	Molecular weight	Source	Stated Mass fraction Purity	CAS no.	Purification method
3-aminopropyl triethoxysilane (TESA)		221.37	Sigma Aldrich Co.	0.99	919-30-2	None
1-(2-Aminoethyl) Piperazine (AEP)		129.21	Sigma Aldrich Co.	0.99	140-31-8	None
Bis(3-aminopropyl)amine (APA)		131.22	Sigma Aldrich Co.	0.98	56-18-8	None
Carbon dioxide (CO ₂)		44.01	Linde India Ltd.	>0.99	367522-96-1	None

solvents for CO₂ capture exhibit several disadvantages ranging from formation of corrosive products, high energy demand for regeneration, lower CO₂ absorption capacity and reaction rates, thermal degradation, instability during regeneration, etc. [8]. Owing to the same reason, a major section of CCS studies focuses on the challenging task of developing novel blended solvents to overcome mentioned issues which cannot be achieved in a single amine solvent. Hence, the concept of combination of various effective solvents offering suitable quality parameters for CO₂ absorption is taken in the literature.

Over the past few years, ionic liquids have received significant attention for CO₂ capture either through absorption or adsorption. Ionic liquids have dual advantages such as thermal stability and extremely low vapour pressures but are also having disadvantages such as high cost, and high viscosities leading to the higher pumping costs in absorption and regeneration columns. To take into account the advantages of ionic liquids and amines in order to provide better CO₂ capture, many researchers have worked for blending optimum amines with ionic liquids [9]. Various intensive studies for CO₂ capture through the use of ionic liquids with amines, other types of solvents such as task specific ILs, reversible ILs (RevILs), phase change solvents, etc. have been attempted and reported elsewhere [8,10–12]. Also, applications of ILs in CO₂ capture using adsorption, IL supported membranes, poly IL membranes, composite membranes as well as successful catalytic conversion of CO₂ to useful products with IL as median have been appreciatively reviewed and reported [13,14]. The results certainly remark a huge potential of identified solvents for CO₂ capture. Conclusively, the blended solvent system, which consists of blending two or more solvents as well as blending with appropriate rate activators, exhibit very promising result in the acid gas separation technology [8–11,15,16].

Novel phase change solvent of triethylenetetraamine hydrobromide ([TETA] Br) and N, N, N', N'', N'''-pentamethyldiethylenetriamine (PMDETA) indicated absorption capacity of 2.631 mol CO₂/ l of the solvent at 303 K and 3:7 M ratio. Analysis of the systems indicated that major CO₂ absorption takes place due to [TETA] Br and PMDETA was approved to be promoting absorption [17]. Shahrom et al. [18] suggested the application of amino acid based polymerized ionic liquids (AAPILs) over task specific ionic liquids (TSILs) and polymerized ionic liquids (PILs) due to increased CO₂ capture efficiency of the former owing to the presence of amine tethered at the anion.

CO₂ absorption capacity of silylated amines such as (3-amino-propyl)-trimethoxysilane (TMSA), (3-aminopropyl)-triethoxysilane (TESA), (3-aminopropyl)-triethylsilane (TEtSA), and (3-aminopropyl)-tripropylsilane (TPSA) which are precursor to corresponding RevILs have been reported [10]. Although, TPSA has shown the better CO₂ absorption capacity but TESA was found to be more thermally stable silylated amine in comparison to others. TESA was found to yield a total CO₂ capture capacity of 14.76 mol of CO₂ per kg of amine. Apart from absorption, earlier instances related to CO₂ adsorption on functionalized graphite oxide [19] and mesoporous silica SBA-15 [20] using TESA have

been also reported in the literature. The studies revealed that the functionalization provided high stable CO₂ adsorption uptakes as well as desorption cycles. The studies further stated that the functionalization of TESA on SBA-15 increased CO₂ adsorption capacity up to 48 mg/g [20]. A combination of TESA and (1-Ethyl-3-methylimidazolium bis (trifluoromethylsulfonyl) imide) have been investigated for developing efficient silica aerogels for CO₂ adsorption [21].

TESA has been selected for the present study owing to its preferential thermal stability and affinity towards CO₂ revealed in the discussed literature. In comparison to the traditional ILs such as imidazolium or phosphonium, RevILs are very cost effective and they also provide the characteristics required such as thermal stability of ILs. Additionally, since the amino group present in TESA is surrounded by single alkyl chain, the CO₂ proton exchange at this junction is less hindered by the alkyl chains, which is expected to provide better CO₂ solubility.

Amongst the various categories of activators, piperazine (PZ) has been explored extensively because of its favorable characteristics such as higher reaction rate, higher equilibrium solubility and lower regeneration temperature compared to conventionally used solvents such as monoethanolamine (MEA). Researchers have blended PZ with N-methyl-diethanolamine (MDEA) or 2-amino-2-methyl-1-propanol (AMP) based solvents owing to its favorable thermodynamic and kinetic properties. However, the usage of concentrated piperazine is limited since it precipitates at lower temperature and lean CO₂ loading. The usage of derivatives of piperazine such as 1-(2-aminoethyl) piperazine (AEP), 1-methyl piperazine (1-MPZ), 2-methyl piperazine (2-MPZ) [22–26] have been also practiced to overcome the constraints revealed by piperazine (PZ). AEP exhibited higher rate constant $3.33 \times 10^4 \text{ m}^3 \cdot \text{kmol}^{-1} \text{ s}^{-1}$ at 303.15 K for aqueous AEP systems which is quite higher than PZ and MEA [27]. Also it can be inferred from the literature corresponding to (AEP + MDEA) system that AEP can be used as a positive enhancer for rate of reaction and equilibrium solubility of CO₂ for the studied solvents [28–30]. The efficiency of another amine based activator, bis (3-amino propyl) amine (APA) in conventional amines and ionic liquids, had been reported elsewhere [29,31]. The selection of APA was based on the higher pKa values of APA in comparison to PZ. The rate of reaction of CO₂ in aq. (APA + AMP) have been found to intensify with the APA concentration. The molecular structural analysis of APA also suggests that it consists of two primary and one secondary amino groups which has a huge contribution for CO₂ equilibrium solubility as well as rate of the reaction.

In this study, we report equilibrium CO₂ solubility in the novel blends of RevIL (TESA) and amine activators. As discussed earlier, TESA blends with either AEP or APA were chosen as innovative solvent due to superior properties. We chose a first principle modified Kent-Eisenberg model to fit VLE data. The major advantage of the modified KE model is its simplicity and few input variables. However, the subsequent output of the model also demonstrates useful insights such as equilibrium constants associated with the proposed reactions, the concentration

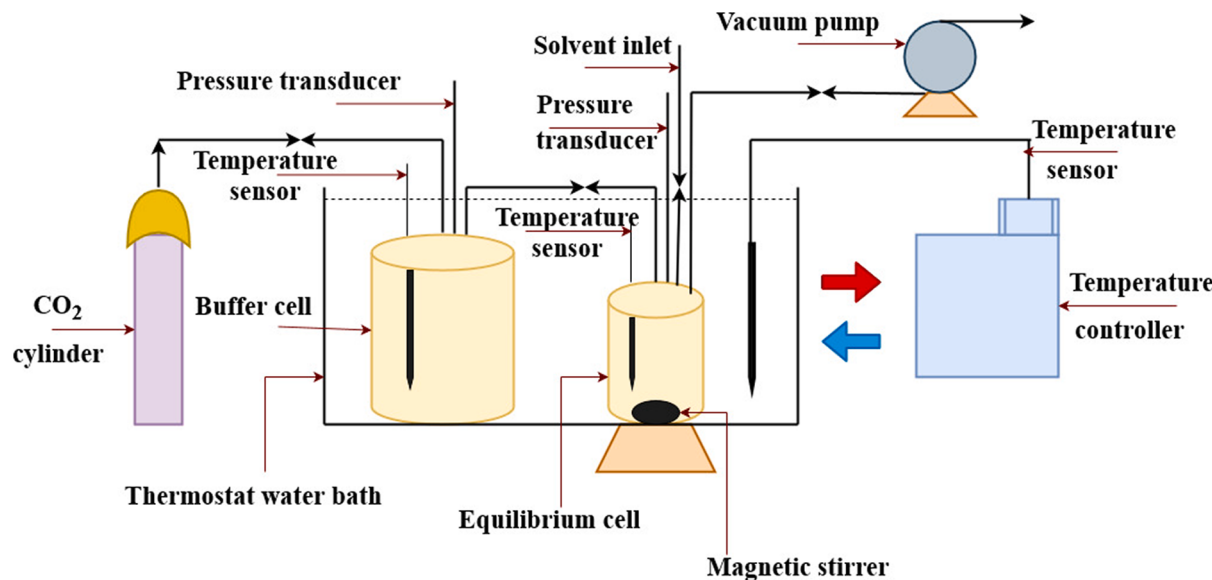


Fig 1. Schematic diagram of experimental set-up.

profiles of the related species as well as pH of the system [31]. In addition, a non-rigorous statistical model is also proposed for correlating CO₂ solubility data. The competency of both the models has also been analyzed. We reasonably envision that the amalgamation of TESA with amine activators AEP and APA may provide better CO₂ loadings in comparison to conventional solvents. By tuning the composition of amine and RevILs, an effective route for CO₂ capture can be achieved. This work demonstrates our effort to achieve such goals.

2. Experimental section

2.1. Materials

3-Aminopropyl triethoxysilane (TESA), 1-(2-Aminoethyl) piperazine (AEP), and Bis (3-aminopropyl) amine (APA) were purchased from Sigma-Aldrich and used with no auxiliary refinement. CO₂ was procured from Linde India Ltd. and used as such. Milipore® water was used throughout. Specification details of the chemicals used under the study are given in Table 1.

2.2. Experimental method

2.2.1. Vapour liquid equilibrium (VLE) measurement

The experimental set-up, methodology and validation of the assembly used to measure VLE have been reported by our research group [29]. Similar, experimental set-up has also been proved to provide accurate CO₂ solubility data in the literature [9,32–34]. These data are also useful in further analyzing the pressure in terms of calculating concentration of various species involved in the reactions, CO₂ cyclic capacity, heat of absorption, etc. However, such calculations cannot be performed while utilizing other methodologies for CO₂ absorption such as wetted wall column method [35], rubotherm magnetic suspension balance [36], etc. The experimental set up is presented in Fig. 1. The total pressure (P^T) prevailing in equilibrium vessel and solvent vapour pressure (P^V) can be used to evaluate the equilibrium partial pressure of CO₂ (P_{CO₂}) at the respective temperature and liquid phase CO₂ loading (α_{CO₂}) [37]. The CO₂ loading (α_{CO₂}) was further estimated as function of temperature and P_{CO₂}.

The total moles of CO₂, n_{CO₂}, transported from buffer vessel to equilibrium vessel is calculated using:

$$n_{CO_2} = \frac{V_b}{R \times T} \times \left(\frac{P_{b1}}{Z_1} - \frac{P_{b2}}{Z_2} \right) \quad (1)$$

where, V_b is volume of the buffer cell, Z₁ and Z₂ are the compressibility factors corresponding to the initial pressure (P_{b1}) and final pressure (P_{b2}) of the buffer cell, respectively. Owing to the gas phase non-ideality at high CO₂ pressures, compressibility factor (Z) is incorporated while calculating moles remaining in the gas phase. Here, 'Z₁' and 'Z₂' are calculated using Peng-Robinson Equation of State (EOS) and the values are used in Eq. (1). The residual CO₂ moles in the gas phase (n^g_{CO₂}) after the establishment of VLE is estimated by Eq. (2).

$$n_{CO_2}^g = \frac{V_g \times P_{CO_2}}{Z_{CO_2} \times R \times T} \quad (2)$$

Where, V_g and Z_{CO₂} symbolize the volume of gas phase and compressibility factor of CO₂ in equilibrium vessel, respectively. Subtraction of liquid volume from equilibrium vessel volume leads to the computation of gas phase volume. The original Peng Robinson Equations of state can be given as follows:

$$P = \frac{R \times T}{v - b} - \frac{a(T)}{v \times (v - b) + b \times (v - b)} \quad (3)$$

The above equation in the form of compressibility factor can be re-written as:

$$z^3 - (1 - B) \times Z^2 + (A - 2 \times B - 3 \times B^2) \times Z - (A \times B - B^2 - B^3) = 0$$

$$A = \frac{a(T) \times P}{R^2 \times T^2} \quad (4a)$$

$$B = \frac{b \times P}{R \times T} \quad (4b)$$

$$a(T) = 0.45724 \times a(T) \times \frac{R^2 \times T_c^2}{P_c} \quad (4c)$$

$$b = 0.07780 \times \frac{R \times T_c}{P_c} \quad (4d)$$

$$a(T) = \left[1 + (0.37646 + 1.4522 \times \omega - 0.26992 \times \omega^2) \left(1 - \sqrt{\frac{T}{T_c}} \right) \right]^2 \quad (4e)$$

where, P, T, v, and R, are pressure, temperature, molar volume and gas

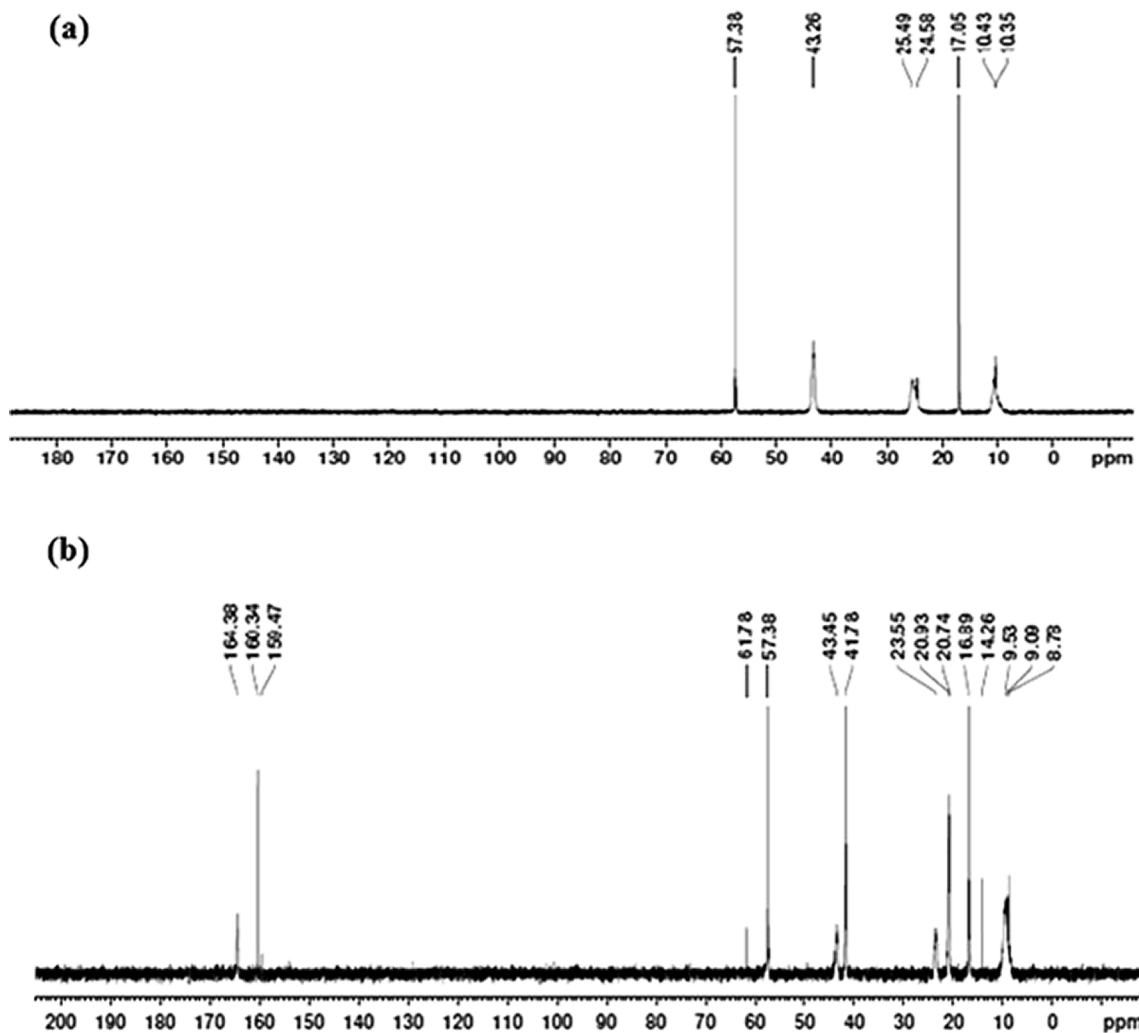


Fig. 2. ^{13}C NMR spectra of 2.432 m aq. TESA solution (a) unloaded (b) CO_2 loaded at 313.2 K.

constant ($8.314 \text{ J mol}^{-1} \text{ K}^{-1}$), respectively. Further, parameters a and b are described in the forms of P_c , critical pressure, T_c , critical temperature and ω , acentric factor of the species.

CO_2 loading (α_{CO_2} in moles of CO_2 / moles of total amine) at equilibrium and particular CO_2 partial pressure (P_{CO_2}) can be evaluated using a vapor and liquid phase mass balance of CO_2 . The expression is given by:

$$\alpha_{\text{CO}_2} = \frac{n_{\text{CO}_2} - n_{\text{CO}_2}^g}{n_{\text{am}}} \quad (5)$$

where, n_{am} indicates the total moles of solvent in the liquid phase.

The estimation of α_{CO_2} is associated with standard uncertainty, which is calculated using error propagation theory [37]. Similar concept of uncertainty estimation has been reported and accepted by many researchers [38,39]. The equation for standard uncertainty calculation is given by:

$$u^2(y) = \sum_{i=1}^n \left(\frac{\partial f}{\partial x_i} \times u(x_i) \right)^2 \quad (6)$$

where, $u(y)$ and $u(x_i)$ are the standard uncertainty corresponding to CO_2 loading and standard uncertainties associated with pressure, temperature, reactor volume, and concentration of ingoing solvent, respectively. Nine solvents with following compositions are studied in the present work at 303.2, 313.2 and 323.2 K: (1) aq. 2.432 M TESA, (2) aq. 1.506 M TESA, (3) aq. 0.797 M TESA, (4) aq. (2.528 M TESA + 0.498 M AEP), (5)

aq. (2.259 M TESA + 0.756 M AEP), (6) aq. (2.044 M TESA + 1.004 M AEP), (7) aq. (2.528 M TESA + 0.499 M APA), (8) aq. (2.259 M TESA + 0.753 M APA) and (9) aq. (2.044 M TESA + 0.991 M APA). Here, 'm' represents mol/kg (molal unit).

2.2.2. FTIR and ^{13}C NMR studies

The ^{13}C NMR study of unloaded and CO_2 loaded solvents at 313.2 K for 2.432 M TESA and (2.259 M TESA + 0.756 M AEP) solvents were carried out using 500 MHz NMR spectrophotometer in D_2O (Model: Ascend, Bruker). Supportingly, these solvents were also considered for FTIR- ATR spectroscopy (Model: Perkin Elmer Inc., Germany) within the wavenumber range of 3000 to 400 cm^{-1} .

3. Proposed chemical reaction

In order to analyze various reaction products and propose a suitable set of reactions, qualitative FTIR and ^{13}C NMR studies of the blends under investigation is carried out. Furthermore, such analysis also gives an understanding of the various bond formations/breakage and intermediates generated during the course of reaction. The reactions proposed are also required while the application of modified KE model. The methodology applied for the analysis is mentioned in section 2.2.2.

The formation of ionic liquid through reaction is verified by ^{13}C NMR spectra analysis of aq. TESA and aq. (TESA + AEP) systems before and after CO_2 absorption (Figs. 2-3), respectively. The ^{13}C NMR of CO_2 loaded 2.432 M aq. TESA and aq. (2.259 M TESA + 0.756 M AEP) are

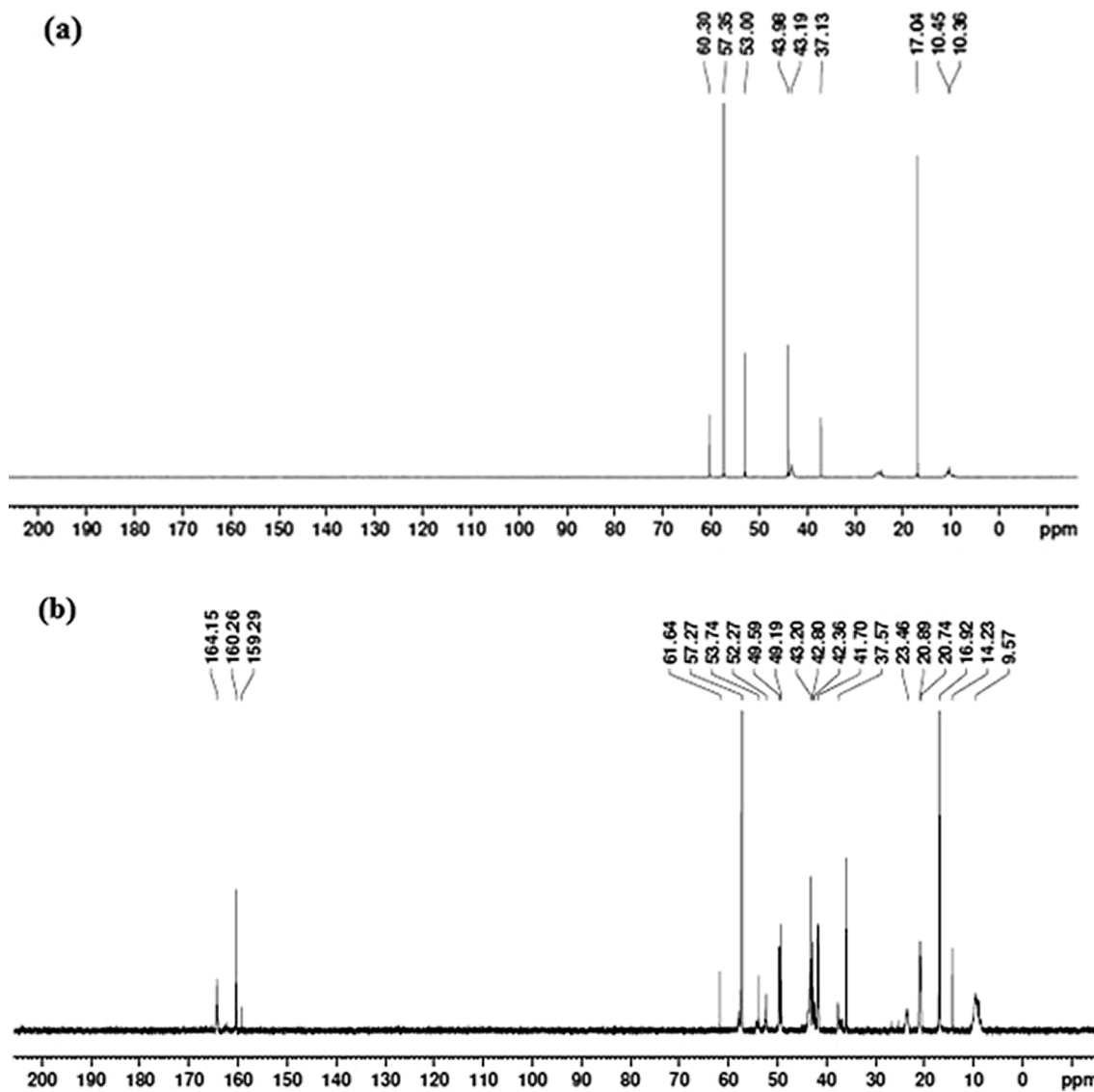


Fig. 3. ^{13}C NMR spectra of aq. (2.259 m TESA + 0.756 m AEP) solution (a) unloaded (b) CO_2 loaded at 313.2 K.

presented in Fig. 2(b) and 3(b). Consequent to carbonyl carbon, three sharp peaks were observed at various positions in the low field range (163–165) ppm which in turn represent the different carbamate groups. Sharp peaks at 164.38 and 164.15 in both cases, indicates the presence of simple primary carbamate and primary carbamate associated to the

dicarbamate, respectively. Similar observations were found for the case of aqueous AEP and aqueous (AEP + PZ) [40]. The formation of carbamate ions while CO_2 reacts in aqueous APA is also confirmed in the literature [31].

The field range on the higher side being (61–10) ppm is observed in

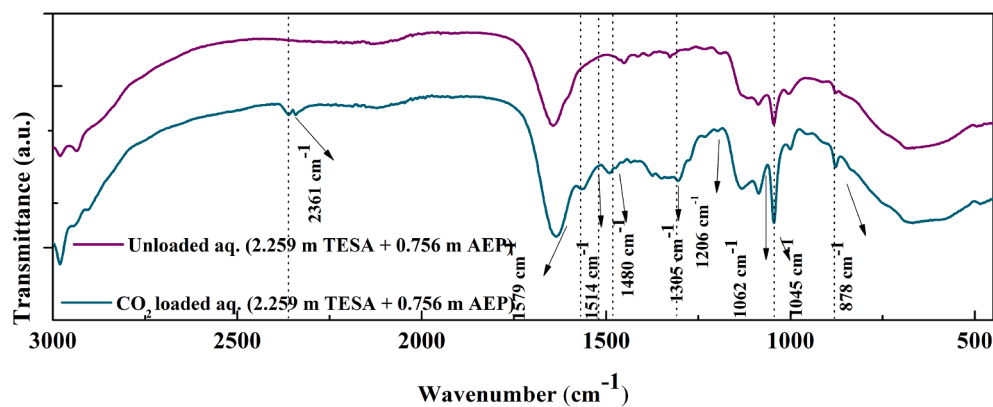


Fig. 4. FTIR-ATR spectra of aq. (2.259 m TESA + 0.756 m AEP) unloaded and CO_2 loaded at 303.2 K.

both the cases of loaded solutions. The highest peak range from (58–34) ppm for loaded aq. AEP systems has been however reported in the literature [40]. Hence, a range of different product formations i.e. reversible ionic liquids are formed over the region from the higher field range of (24–10) ppm. The ^{13}C NMR spectrum of loaded TESA is compared with the literature [41]. According to the literature work, following peaks were found in the ^{13}C NMR spectra of TESA ionic liquid: 162.5, 57.7, 44.1, 41.5, 23.7, 21.3, 17.9, 7.6 and 7.4. The ^{13}C NMR spectra of CO_2 loaded aq. TESA and aq. (TESA + AEP) systems have shown similar peaks with a small deviation (Fig. 2(b)-3(b)). The conceivable reasons for this shift are either (i) due to the presence of water in the present case or (ii) due to the temperature divergence at which absorption of CO_2 is carried out. The comparison of ^{13}C NMR spectra between the literature and present work confirmed the formation of reversible TESA based ionic liquid.

FTIR-ATR has been carried out to analyze the variations in different associated bonds in the reactants which results in formation of proposed products. The FTIR analysis of CO_2 loaded and unloaded aq. (2.259 m TESA + 0.756 m AEP) solution is carried out in the present work (Fig. 4). A new peak at 2361 cm^{-1} was observed which concludes the asymmetric stretching due to dissolved CO_2 . Also, the bands at 1579, 1514 and 1480 cm^{-1} are observed for loaded solvent in comparison with unloaded one, which can be assigned to COO^- asymmetric and symmetric stretching, respectively. However, the peaks at 1305 and 1206 cm^{-1} are anticipated to NCOO^- stretching vibrations of carbamate species and C (O)-O stretching vibrations. Due to the protonation of TESA and AEP, the peaks of C-N and C-O observe a shift from 1075 to 1062 cm^{-1} and 1043 to 1045 cm^{-1} , respectively. Similarly, the peaks at 878 cm^{-1} can be attributed to C-NH₂ twisting for AEP [42–44].

Through the results of ^{13}C NMR and FTIR, it can be concluded that TESA gets reacted to CO_2 forming anion and cation. Additionally, the comparison of the results of various peaks of the two analysis indicated the reversible nature of the ionic liquid associated with TESA. Hence, the proposed reaction scheme for CO_2 solubility in pure TESA is as given below:

Moreover, while the CO_2 solubility in aq. (TESA + AEP/APA) takes places, the liquid phase during the process exhibits various simultaneous reactions. Majorly, it consists of protonation of both TESA and APA/AEP amine activators, carbamate formation by APA/AEP and other reactions. The bicarbamate formation of AEP is however not significant [27] since at higher CO_2 loading bicarbonate is the major product of (AEP- CO_2) reaction [45]. The carbamate formation for reaction between TESA and CO_2 has been already reported in the literature [19,46,47] and the same has been confirmed in the present study.

The equilibrium reactions for (TESA + $\text{H}_2\text{O} + \text{CO}_2$), (TESA + AEP + $\text{H}_2\text{O} + \text{CO}_2$) and (TESA + APA + $\text{H}_2\text{O} + \text{CO}_2$) have been proposed using reactions R₁ to R₁₀:

Physical Solubility



Dissociation of bicarbonate ion



Formation of bicarbonate ion



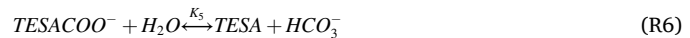
Dissociation of water



Deprotonation of TESA



Carbamate hydrolysis of TESA



Deprotonation of AEP



Carbamate hydrolysis of AEP



Deprotonation of APA



Carbamate hydrolysis of APA



where, each term has their usual meaning with K₁, K₂, K₃, K₄, K₅, K₆, K₇, K₆', and K₇' being the equilibrium constants associated with respective reactions (R₂-R₁₀).

4. Vapour liquid equilibrium modeling

The literature provides the prediction of CO_2 solubility in amine or ionic liquid based solutions using various models based on thermodynamics of the systems such as e-NRTL [37], Peng-Robinson Equation of State (EOS) [48], Deshmukh Mather [49,50], and RETM model [51]. The EoS based models usually provide a better prediction capability in pure solvents. However, for CO_2 solubility in ILs or blended solvents, these models have proved to yield less accuracy [32,52]. Comparatively, modified KE model is quite simple and require less computation time [53,54]. Hence, modified KE model has been considered here to correlate the CO_2 solubility data in aqueous blends [55–58]. Furthermore, based on the dependence of CO_2 solubility with respect to temperature, pressure, concentration of TESA and AEP/APA, a new non-rigorous and non-linear statistical model has also been proposed. Similar models reported in the literature have proven to provide improved precise estimate of CO_2 solubility [52,59].

4.1. Modified Kent-Eisenberg model

Absorption of CO_2 in the blended solutions depends on the achievement of both, phase and chemical equilibrium. The physical solubility of CO_2 is usually due to the weak van der Walls forces of attraction which here is presented by Henry's law. Reversible reactions in the liquid phase are explained using chemical equilibrium. In the present work, the non-ideality in the vapor phase is incorporated using fugacity coefficient in the modified KE model.

In modified KE model, activity coefficients (γ_i) of all species in liquid phase are taken as unity. The reactions R₁-R₆ are applicable for CO_2 solubility in the system of aqueous TESA whereas reactions R₁-R₁₀ are valid for CO_2 solubility in (TESA + AEP/APA) systems. The concentration of species based on apparent equilibrium constants of R₂-R₁₀ are presented as:

$$K_1 = \frac{[\text{CO}_3^{2-}][\text{H}^+]}{[\text{HCO}_3^-]} \quad (7)$$

$$K_2 = \frac{[\text{HCO}^{3-}][\text{H}^+]}{[\text{CO}_2]} \quad (8)$$

$$K_3 = [\text{H}^+][\text{OH}^-] \quad (9)$$

$$K_4 = \frac{[\text{TESA}][\text{H}^+]}{[\text{TESAH}^+]} \quad (10)$$

$$K_5 = \frac{[TESA][HCO_3^-]}{[TESACOO^-]} \quad (11)$$

$$K_6 = \frac{[AEP][H^+]}{[AEPH^+]} \quad (12)$$

$$K_7 = \frac{[AEP][HCO_3^-]}{[AEPCOO^-]} \quad (13)$$

$$K'_6 = \frac{[APA][H^+]}{[APAH^+]} \quad (14)$$

$$K'_7 = \frac{[APA][HCO_3^-]}{[APACOO^-]} \quad (15)$$

where, the square [] brackets indicate the concentration of the chemical species.

Vapor phase equilibrium, which dictates the relationship between CO₂ partial pressure P_{CO₂} at equilibrium and physically dissolved CO₂ concentration [CO₂], is expressed by Henry's law as presented in Eq. (16).

$$P_{CO_2} = H_{CO_2} \times [CO_2] \quad (16)$$

The general mass and charge balance of various molecular and ionic species present in the liquid phase can be expressed as:

TESA Balance:

$$[TESA]_r = M_1 = [TESA] + [TESAH^+] + [TESACOO^-] \quad (17)$$

CO₂ Balance for aqueous TESA system:

$$\alpha_{CO_2} \times (M_1) = [CO_2] + [HCO_3^-] + [CO_3^{2-}] + [TESACOO^-] \quad (18)$$

where α_{CO₂} is the CO₂ loading and M₁, represents initial TESA molar concentration.

Charge Balance for aqueous TESA system:

$$[H^+] + [TESAH^+] = [HCO_3^-] + 2 \times [CO_3^{2-}] + [OH^-] + [TESACOO^-] \quad (19)$$

The system of Eqs. (7) - (15) and (17) - (19) can be utilized to develop polynomial equations which are formed in terms of [H⁺]. The equation hence formed for systems considered associated with the coefficients can be given as follows:

For aqueous TESA system:

$$A_1 \times [H^+]^5 + B_1 \times [H^+]^4 + C_1 \times [H^+]^3 + D_1 \times [H^+]^2 + E_1 \times [H^+] + F_1 = 0 \quad (20)$$

where,

$$A_1 = K_5 \quad (20a)$$

$$B_1 = K_5 \times (K_4 + M_1) \quad (20b)$$

$$C_1 = K_2 \times [CO_2] \times (K_4 - K_5) - K_5 \times K_3 \quad (20c)$$

$$D_1 = -K_2 \times K_5 \times [CO_2](K_4 + 2 \times K_1) - K_3 \times K_4 \times K_5 \quad (20d)$$

$$E_1 = -K_2 \times K_4 \times [CO_2] \times (K_2 \times [CO_2] + 2 \times K_1 \times K_5 + K_3) \quad (20e)$$

$$F_1 = -2 \times K_1 \times K_2^2 \times K_4 \times [CO_2]^2 \quad (20f)$$

Furthermore, the modified form of loading equation for the aqueous TESA system is derived as:

$$\alpha_{CO_2} = \frac{\varphi_{CO_2} \times P_{CO_2}}{(H_{CO_2} \times M_1)} \left[1 + \frac{K_2}{[H^+]} + \frac{K_1 \times K_2}{[H^+]^2} + \frac{M_1 \times K_2 \times K_4}{K_4 \times K_5 \times [H^+] + K_5 \times [H^+]^2 + K_2 \times K_4 \times \left[\frac{P_{CO_2}}{H_{CO_2}} \right]} \right] \quad (21)$$

where φ_{CO₂} is fugacity coefficient contributing to the non-ideality in the gas phase.

Fugacity coefficient of an acid gas at its partial pressure is estimated using virial EoS as given below:

$$\ln(\varphi_{CO_2}) = \frac{B_{ii} \times P}{R \times T} \int_0^P dP \quad (22)$$

$$\text{or, } \ln(\varphi_{CO_2}) = \frac{B_{ii} \times P}{R \times T}$$

Where, B_{ii} indicates the interactions between paired molecules and can be considered using Virial EOS.

$$\ln(\varphi_{CO_2}) = \frac{B_{ii} \times P_C \times P_R}{R \times T_C \times T_R} \quad (22a)$$

Including the acentric factor in the above Eq. (22), it can be written as:

$$\ln(\varphi_{CO_2}) = (U_1 + \omega \times U_2) \times \frac{P_R}{T_R} \quad (22b)$$

where,

$$U_1 = 0.083 - \frac{0.422}{T_R^{1.6}} \quad (22c)$$

$$U_2 = 0.139 - \frac{0.172}{T_R^{4.2}} \quad (22d)$$

here, P_R, P_C, T_R, T_C and ω are reduced pressure, critical pressure, reduced temperature, critical temperature and acentric factor which is 0.239 for CO₂, respectively. The values for P_C and T_C are taken as 73.87 bar and 304.2 K, respectively. α_{CO₂} is estimated using Eq. (21) which needs the real root of [H⁺] obtained from Eq. (20). In modified KE model, the equilibrium constant (K₁ - K₃) can be measured as function of temperature as given below:

$$\ln K_i = a_i + \frac{b_i}{T} + c_i \times \ln T \quad (23)$$

where a_i, b_i and c_i are coefficients of Eq. (23) are taken from the literature [37].

The physical solubility represented by Henry's constant, H_{CO₂} can be given as below [53].

$$\ln H_{CO_2} (kPa.m^3/kmol) = 20.2669 - \frac{1.3830 \times 10^4}{(T/K)} + \frac{0.0691 \times 10^8}{(T/K)^2} - \frac{0.0156 \times 10^{11}}{(T/K)^3} + \frac{0.0120 \times 10^{13}}{(T/K)^4} \quad (24)$$

The equations related to the modified KE model are combination of various linear and non-linear equations, which necessarily be solved simultaneously. For the same, an essential requirement stands to be optimization technique along with a specific objective function, which in the present case is taken as error deviation. The equilibrium constants K₄, K₅, K₆, K₇, K'₆, and K'₇ which are associated to the deprotonation and carbamate hydrolysis reactions of TESA, AEP, and APA, respectively, are obtained as a function of P_{CO₂}, T and solvent concentration using regression analysis in MATLAB (R17). The necessary technique used for

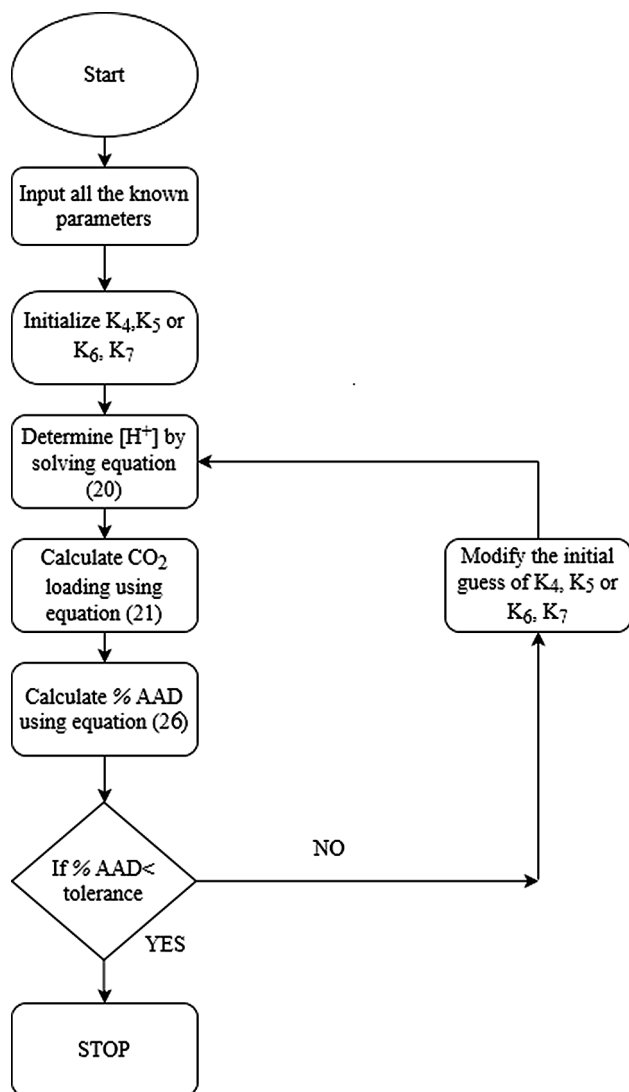


Fig. 5. Regression algorithm for estimation of equilibrium constants from experimental CO₂ loading data.

non-linear regression analysis is presented in Fig. 5.

4.2. Non-rigorous statistical model (N_1)

Statistical regressive models have been of interest in the past owing to the ease of calculations of the interaction parameters i.e. the coefficients associated with the model [52,60,61]. In addition, these models also proved to provide better prediction capabilities over a wide range of reaction conditions. Unlike the first principle or deterministic models, these models require less input data. Considering this, here a non-rigorous statistical non-linear model is proposed as equation (25).

$$\alpha_{CO_2} = d_0 + (d_1 \times (\log(P_{CO_2}))) + \left(d_2 \times \left(\frac{1}{T} \right) \right) + (d_3 \times (M)) + \left(d_4 \times \left(\frac{\log(P_{CO_2}) \times M}{T} \right) \right) + \left(d_5 \times \left(\frac{\log(P_{CO_2}) \times M^2}{T} \right)^2 \right) \quad (25)$$

where, α_{CO_2} , P_{CO_2} , T , and M are equilibrium CO₂ loading in mol of CO₂ per mol of solvent, CO₂ partial pressure (kPa), temperature (K) and total molarity of the solvent in kmol.m⁻³, respectively. d_0 , d_1 , d_2 , d_3 , d_4 and d_5 are the coefficients. The non-linear regression is done in MATLAB (R17).

The precision of new model and modified KE model for prediction of

the CO₂ loading data sets of all the blends is analyzed using the calculation of %AAD as stated below:

$$\text{Average absolute deviation } (\%AAD) = \frac{1}{N} \left(\sum_{i=1}^N \frac{|Y_i^{exp} - Y_i^{mod}|}{Y_i^{exp}} \right) \times 100 \quad (26)$$

where, N , Y_i^{exp} and Y_i^{mod} represents the number of data points, experimental value of α_{CO_2} and modeled value of α_{CO_2} , respectively.

5. Results and discussion

5.1. Effect of reaction parameters on CO₂ solubility

The equilibrium VLE data is an essential measurement since it provides an understanding of the distribution of various species involved in the reaction over different phases. The CO₂ solubility measured in the present work included both: physical and chemical solubility, which has been presented in terms of α_{CO_2} i.e. mol of CO₂ per mol of solvent as a function of temperature, solvent concentration and CO₂ partial pressure (Figs. 6 and 7). The maximum estimated uncertainty of CO₂ loading is calculated to be 0.038.

The CO₂ loading was observed to increase with P_{CO₂} and solvent concentration at constant temperature for all the blends under study (Figs. 6-7). This is owing to the rise in P_{CO₂}, the kinetic energy between CO₂ gas molecules and liquid surface increases. Further, α_{CO_2} is found to decrease with increase in temperature at constant pressure and solvent concentration [9,15]. However, in the present case, the dependency of CO₂ loading with temperature is not uniform. The highest loading in case of (2.528 m TESA + 0.498 m AEP) was observed at 313.2 K whereas for (2.259 m TESA + 0.753 m APA) system, the highest α_{CO_2} was found at 323.2 K [10,62-64].

It was observed that the optimum temperature for the simultaneous absorption of CO₂ and formation of ionic liquids is at 313.2 K for aqueous (TESA + AEP) system. The reason may be attributed to the possible pronounced solvent-solute interactions at the corresponding temperature. However, on further increasing the temperature at 323.2 K, the solvent-solute interaction decreases due to the reversible nature of the ionic liquids formed. One of the leading conclusions is that aqueous TESA system yields the highest CO₂ loading at 303.2 K but by addition of activators AEP and APA to the aqueous TESA system, the highest CO₂ loading were found at higher temperatures [62-64].

The VLE data has been correlated using modified KE model where the coefficients of the equilibrium constants, K₄, K₅, K₆, K_{6'}, K₇ and K_{7'} have been evaluated. A non-linear optimization method with the objective function as Eq. (26) was employed to reduce the inaccuracy between experimental and predicted values. The equilibrium constants (K₄, K₅, K₆, K_{6'}, K₇ and K_{7'}) discussed in terms of concentration of solvents, temperature, and P_{CO₂} can be presented as:

$$K_4(\text{or}/K_6\text{or}/K_6') = g + (h \times M) + (k \times T) + (l \times M \times T) + (n \times T^2) + (p \times P_{CO_2}) + (q \times P_{CO_2}^2) \quad (27)$$

$$K_5(\text{or}/K_7\text{or}/K_7') = g + (h \times M) + (k \times T) + (l \times M^2) + (n \times M \times T) + (p \times T^2) + (q \times P_{CO_2}) + (r \times P_{CO_2}^2) \quad (28)$$

where, g , h , k , l , n , p , q and r are the coefficients associated with the equilibrium constants (K₄/K₅/K₆/K₇/K_{6'}/K_{7'}) and are found by optimization.

CO₂ loading (α_{CO_2}) was observed to increase with the rise in AEP/APA concentration in respective solvent systems (Figs. 6 and 7). For instance, at pressure of approximately 180 kPa and at 303.2 K, α_{CO_2} was found to increase substantially by around 20% and 11% for

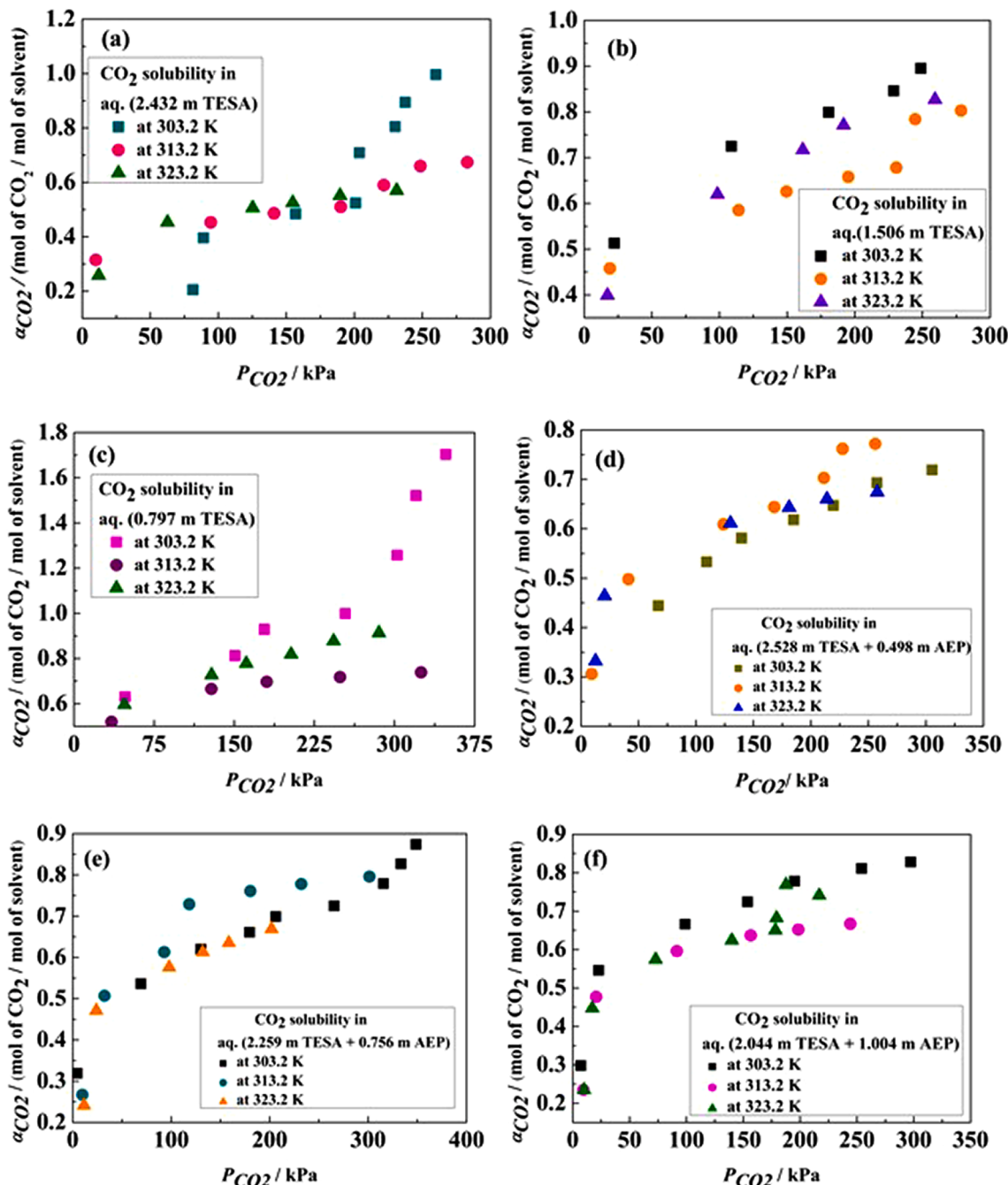


Fig. 6. Experimental equilibrium CO_2 solubility in (a) aq. (2.432 m TESA) (b) aq.(1.506 m TESA) (c) aq. (0.797 m TESA) (d) aq. (2.528 m TESA + 0.498 m AEP) (e) aq. (2.259 m TESA + 0.756 m AEP) and (f) aq.(2.044 m TESA + 1.004 AEP) as a function of temperature ('m' signifies 'mol/kg').

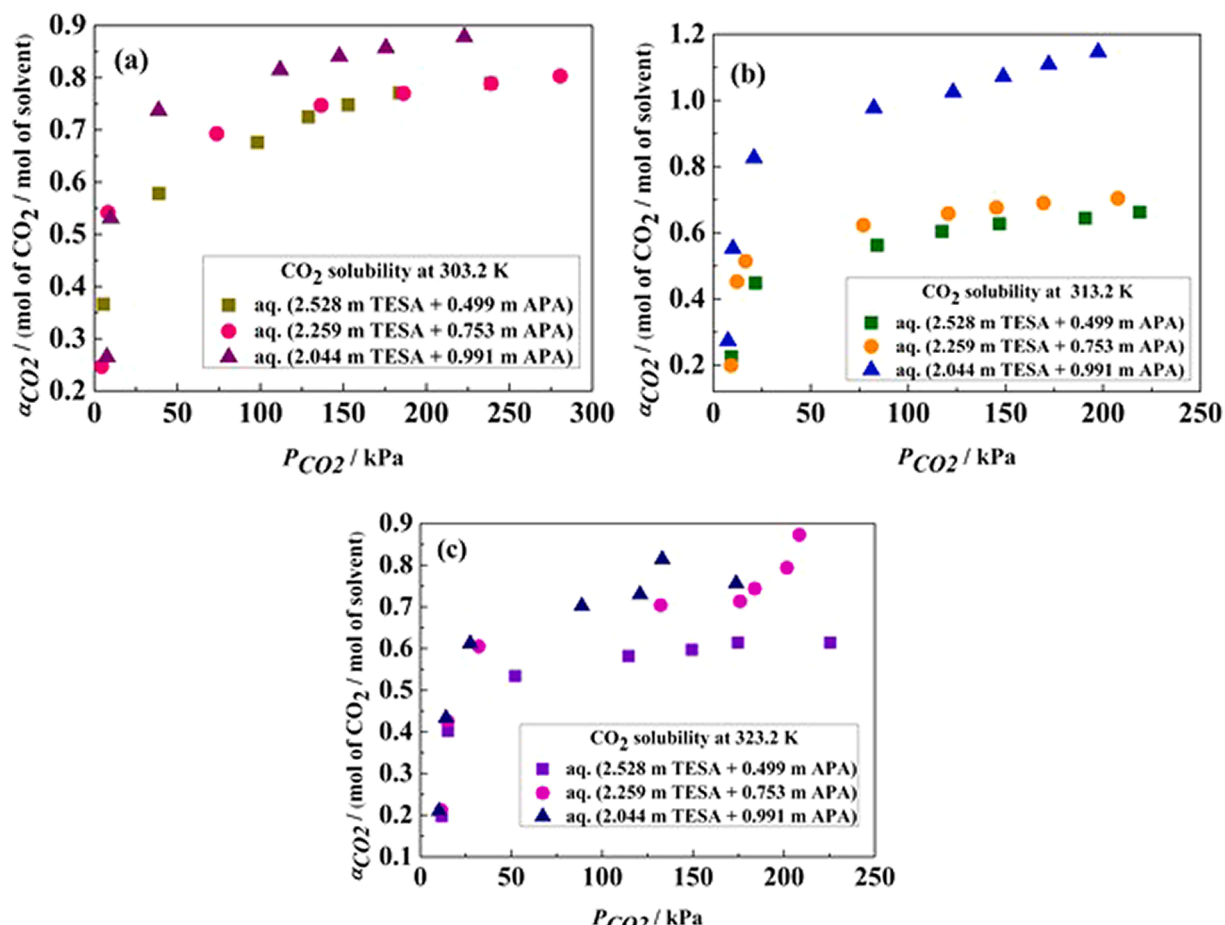


Fig. 7. Experimental equilibrium CO₂ solubility in aq. (TESA + APA) (a) at 303.2 K, (b) at 313.2 K (c) at 323.2 K as a function of concentration ('m' signifies 'mol/kg').

Table 2
Coefficients of the equilibrium constants estimated in the present work.

K _i /kmol. m ⁻³	K ₄	K ₅	K ₆	K ₇	K _{6'}	K _{7'}
g	-1.016 × 10 ⁻¹⁰	2.216 × 10	-2.494 × 10 ⁹	2.948 × 10	8.963 × 10 ⁹	1.475 × 10
h	1.156 × 10 ⁻⁸	-4.035 × 10 ⁻³	2.278 × 10 ⁻¹²	-4.626 × 10 ⁻¹	2.264 × 10 ⁻¹⁶	-1.373 × 10
k	-2.110 × 10 ⁻¹¹	-7.911 × 10 ⁻³	-2.566 × 10 ⁻¹²	-1.126	-5.547 × 10 ⁻¹¹	1.404 × 10
l	1.906 × 10 ⁻¹²	1.534 × 10 ⁻³	2.224 × 10 ⁻¹³	-3.637 × 10 ⁻¹	4.076 × 10 ⁻¹²	1.659 × 10
n	1.230 × 10 ⁻¹³	8.261 × 10 ⁻³	1.019 × 10 ⁻¹³	1.122	1.222 × 10 ⁻¹⁴	2.813 × 10 ⁻¹
p	-7.094 × 10 ⁻¹²	-2.199 × 10 ⁻⁴	-5.604 × 10 ⁻¹¹	-2.843 × 10 ⁻²	-6.469 × 10 ⁻¹¹	-1.409 × 10 ³
q	-3.639 × 10 ⁻¹⁸	7.028 × 10 ⁻²	-5.885 × 10 ⁻²⁴	2.201	-5.248 × 10 ⁻¹⁸	1.155 × 10 ²
r	- × 10 ⁻⁴	-2.161 -	-	-2.408 × 10 ⁻²	-	-3.480 × 10

corresponding increment in the activator concentration from 0.499 m to 0.991 m for AEP and APA, respectively. Also, comparative evaluation of CO₂ loading in 2.432 m aq. TESA, along with (2.528 m TESA + 0.498 m AEP) and (2.528 m TESA + 0.499 m APA) also showed an increase of CO₂ loading by 17.0% and 49.7%, respectively at 303.2 K. This further indicates that APA is a better activator for CO₂ absorption in aq. TESA compared to AEP. The obtained analysis is owing to the more amino groups attached to APA molecule in comparison to AEP. Hence, the

Table 3
Coefficients of the proposed model N₁ estimated in the present work.

Predicted Coefficients	aq. TESA	aq.(TESA + AEP)	aq.(TESA + APA)
d ₀	-4.232	-1.205	-8.204
d ₁	0.402	0.149	0.224
d ₂	1.107 × 10 ³	2.686 × 10	1.725 × 10 ²
d ₃	0.630	0.643	3.843
d ₄	-8.963 × 10	-1.240 × 10	2.288 × 10
d ₅	8.136 × 10 ²	1.866 × 10 ²	-7.848 × 10 ²
100 AAD	16.37	8.55	14.49
SD	0.32	0.21	0.27

probability of CO₂ molecule is more to react with APA molecule than AEP.

The equilibrium constants obtained through KE model (Table 2) were in turn used to predict the CO₂ loading. The calculated % AAD for aqueous TESA, (TESA + AEP) and (TESA + APA) systems are 12.9, 13.2, and 16.2, respectively.

5.2. Co-relation using model (N₁)

The experimental CO₂ loading data is further co-related using model N₁ with respect to P_{CO₂}, T and molarity of the solvents associated as described in Eq. 25. The % AAD for aq. TESA, aq. (TESA + AEP) and aq. (TESA + APA) are estimated to be 16.4, 8.6 and 14.5, respectively. The coefficients of non-linear regression are presented in Table 3. Both the models i.e. modified KE and N₁ are found to be quite competitive in predicting CO₂ solubility. The major advantage of modified KE over N₁

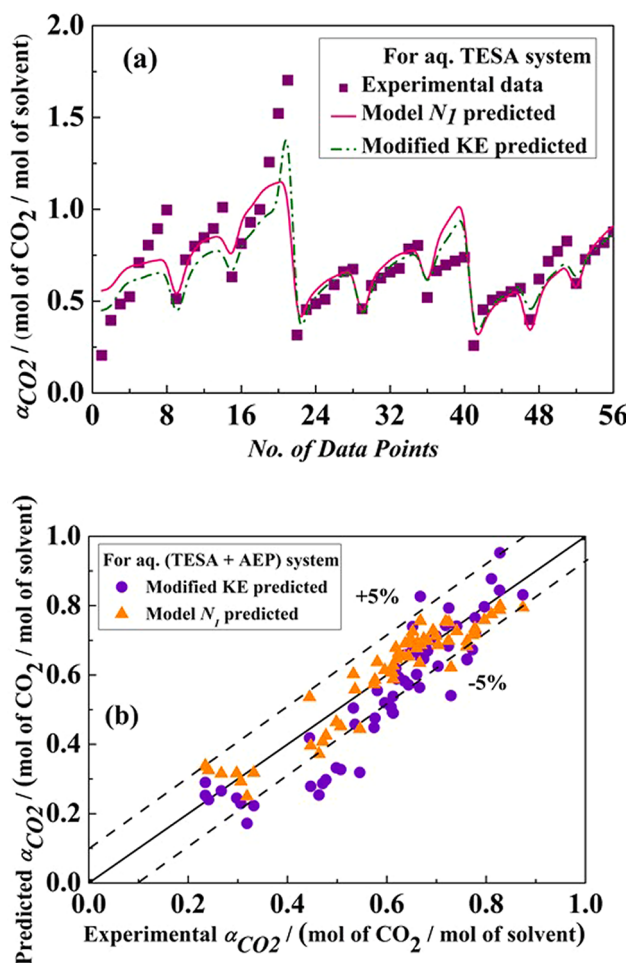


Fig. 8. Comparison of experimental and modeled CO_2 loading values (a) aq. TESA system: cross plot (b) aq. (TESA + AEP): parity plot.

model is that the data obtained through former can be further analyzed for prediction of liquid phase speciation and pH of the systems. The experimental and modeled values are for aq. TESA and aq. (TESA + AEP) systems are observed to be in fine concurrence with each other using both the models (Fig. 8(a-b)).

5.3. Liquid phase speciation and estimation of pH

The equilibrium concentrations of different constituent species available in the liquid phase are further predicted in variation with CO_2 loading using modified KE model applied to all the systems. The concentration profiles of diverse species for CO_2 loaded (1.506 m TESA) at 303.2 K, (2.259 m TESA + 0.753 m APA) at 323.2 K and (2.259 m TESA + 0.756 m AEP) at 303.2 K have been represented in Fig. 9(a), 9(b) and 9(c), respectively.

The concentration of the reactive species TESA, AEP and APA have a decreasing concentration attributable to the reason of their conversion to intermediate species or final products such as bicarbonates, protonated species or carbamates associated to TESA/AEP/APA. Also, compared to TESA, AEP/APA witnessed a more steep decrease in the concentrations as a function of CO_2 loading indicating AEP/APA to be a limiting reactant for CO_2 solubility reaction. Subsequently, TESA depart slowly but surely with α_{CO_2} and thereby key reaction products are protonated TESA and bicarbonate ion. The dissociation and formation of $[HCO_3^-]$ to CO_3^{2-} species (R_2-R_3) leads to intermediate profile of both the species with a very low concentrations as a function of CO_2 loading (Fig. 9(a-c)). Estimation of pH is important since it is one of the important design

parameters for absorption / stripping towers. The reaction products of the considered systems are customarily found to be in the pH range of (7–12) [22]. In the present work, modified KE model is therefore used to analyze pH of blended solvent systems as a function of CO_2 loading. For aq. (2.528 m TESA + 0.499 m APA) system, the highest pH was observed at a low temperature of 303.2 K (Fig. 9(d)). High H^+ ions at high temperature and loading leads to the decrease in pH.

5.4. Comparison of CO_2 solubility with literature

The competence of the studied solvents with literature is shown in Fig. 10(a-d). Due to the limitations of the available literature over the present studied concentration range, the nearest available literature is being considered [29,65–70]. The CO_2 solubility in aq. (2.044 m TESA + 1.044 m AEP) and aq. (2.044 m TESA + 0.991 m APA) is compared with aq. ([bmim] [Ac] + AEP/APA) (2.0 + 1.0) m at 303.2 K [29]. As shown in Fig. 10(a), aq. (TESA + APA) has better performance in comparison to all other three blends. Also, both TESA based blends are found to outperform in comparison to [bmim] [Ac] based solvents with almost similar molal composition. Additionally, single aqueous amines are being compared with the performance of 2.432 m aq. TESA ≈ 35 wt% in Fig. 10(c). At elevated P_{CO_2} , performance of aq. TESA is better than aq. MEA, methyl4-morpholine (2.5 M) and pyridine (2.5 M). The higher values of α_{CO_2} can be the results of development of unstable carbamates formed during the reaction between CO_2 and TESA in presence of water. Further, these carbamates may go through hydrolysis reaction to structure free amine molecules and bicarbonate ions which results in

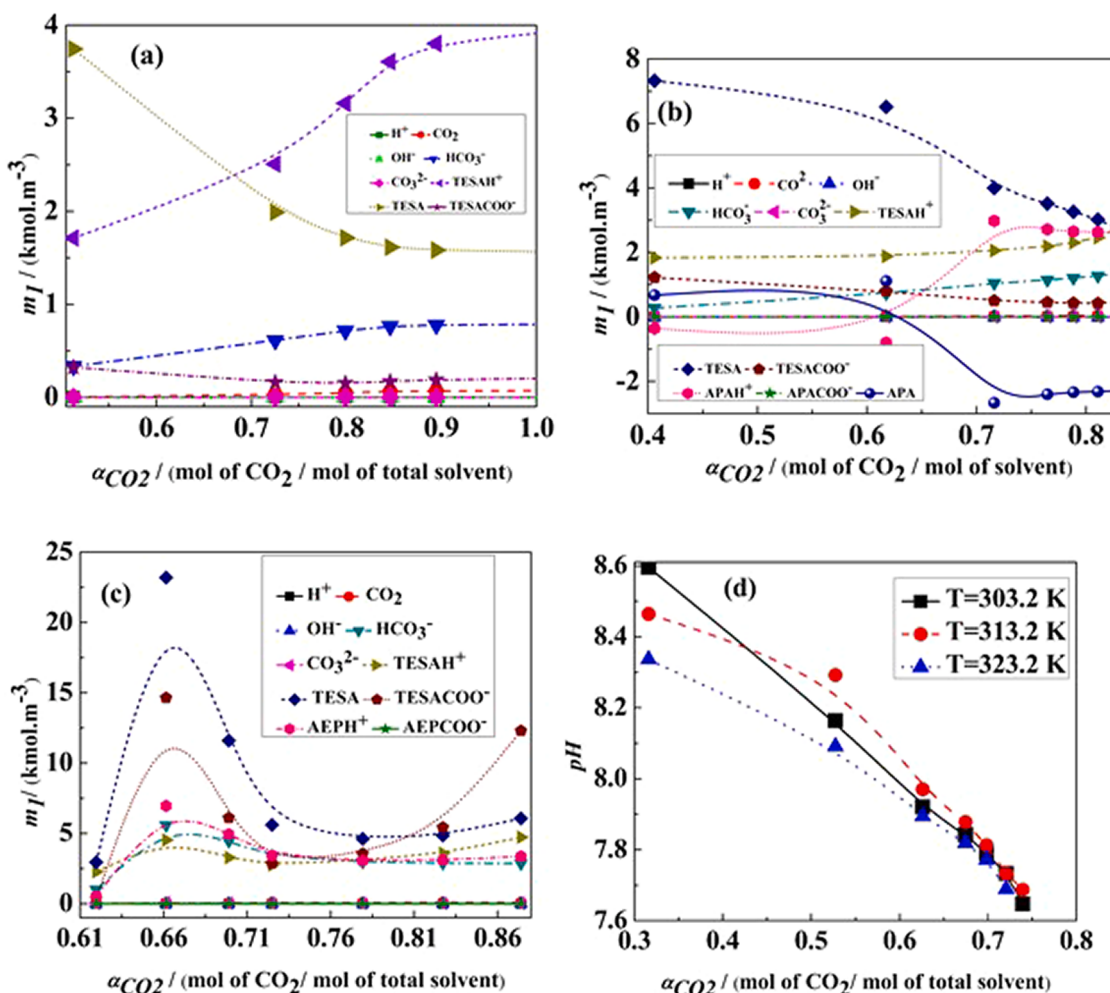


Fig. 9. Model predicted equilibrium liquid phase concentration of various species in CO_2 loaded (a) aq. (TESA) (1.506 m) at $T = 303.2 \text{ K}$ (b) aq. (2.259 m TESA + 0.753 m APA) at $T = 323.2 \text{ K}$ (c) aq. (2.259 m TESA + 0.756 m AEP) at $T = 303.2 \text{ K}$ (d) Modified KE predicted pH in aq. (2.528 m TESA + 0.499 m APA) at 303.2 K, 313.2 K and 323.2 K as a function of CO_2 loading ('m' signifies 'mol/kg').

amplification of α_{CO_2} subsequently. In addition to this, the formation of reversible ionic liquid in TESA also leads to rise in CO_2 loading in comparison with MEA. Thus, in general, it can be concluded that while increasing the concentration of TESA and AEP/APA shall significantly improve the CO_2 solubility while forming reversible ILs.

6. Conclusions

CO_2 solubility in aqueous based reversible ILs enhanced by amine activators viz. AEP and APA were studied over a wide range of experimental conditions. The formation of ILs during the reaction is confirmed by ^{13}C NMR of the loaded solvents. FTIR analysis of loaded and unloaded solvents emphasizes on formation of various bonds while TESA/AEP/APA reacts with CO_2 . Additionally, the analysis confirmed the formation of various carbamate, bicarbonate and protonated ions during reaction of CO_2 with TESA and AEP/APA. The experimental results clearly indicate that CO_2 solubility increases with respect to rise in both partial pressure of CO_2 and concentration of activators in solvent blends. Further quantifying the results signifies that inclusion of $\approx 0.5 \text{ m}$ AEP/APA to 2.432 m aq. TESA intensified the CO_2 solubility by 17 and 50%, respectively at 303.2 K. This indicates that APA is a better activator compared to AEP. The equilibrium constants associated with various reactions as a function of P_{CO_2} , solvent concentration and temperature of absorption were estimated using nonlinear-regression analysis. The efficient prediction capability of modified KE model can be inferred

through the calculated % AAD which are 12.9, 13.2, and 16.2%, for aq. TESA, aq. (TESA + AEP) and aq. (TESA + APA), respectively. A non-linear statistical model is proposed for correlating α_{CO_2} with various reaction parameters and was found to have good competency. The speciation and pH as function of CO_2 loading were estimated by means of modified KE model. A comparison of performance of activated TESA with activated [bmim] [Ac] yielded that the former is having better CO_2 absorption capacity. Hence, an assessment of CO_2 solubility data with literature suggests that the considered solvents have very good potential for post combustion CO_2 capture.

CRediT authorship contribution statement

Sweta C Balchandani: Methodology, Investigation, Validation, Software, Writing - original draft. **Bishnupada Mandal:** Supervision, Conceptualization, Writing - review & editing. **Swapnil Dharaskar:** Co-Supervision, review and editing.

Declaration of Competing Interest

The authors declare that they have no known competing financial interests or personal relationships that could have appeared to influence the work reported in this paper.

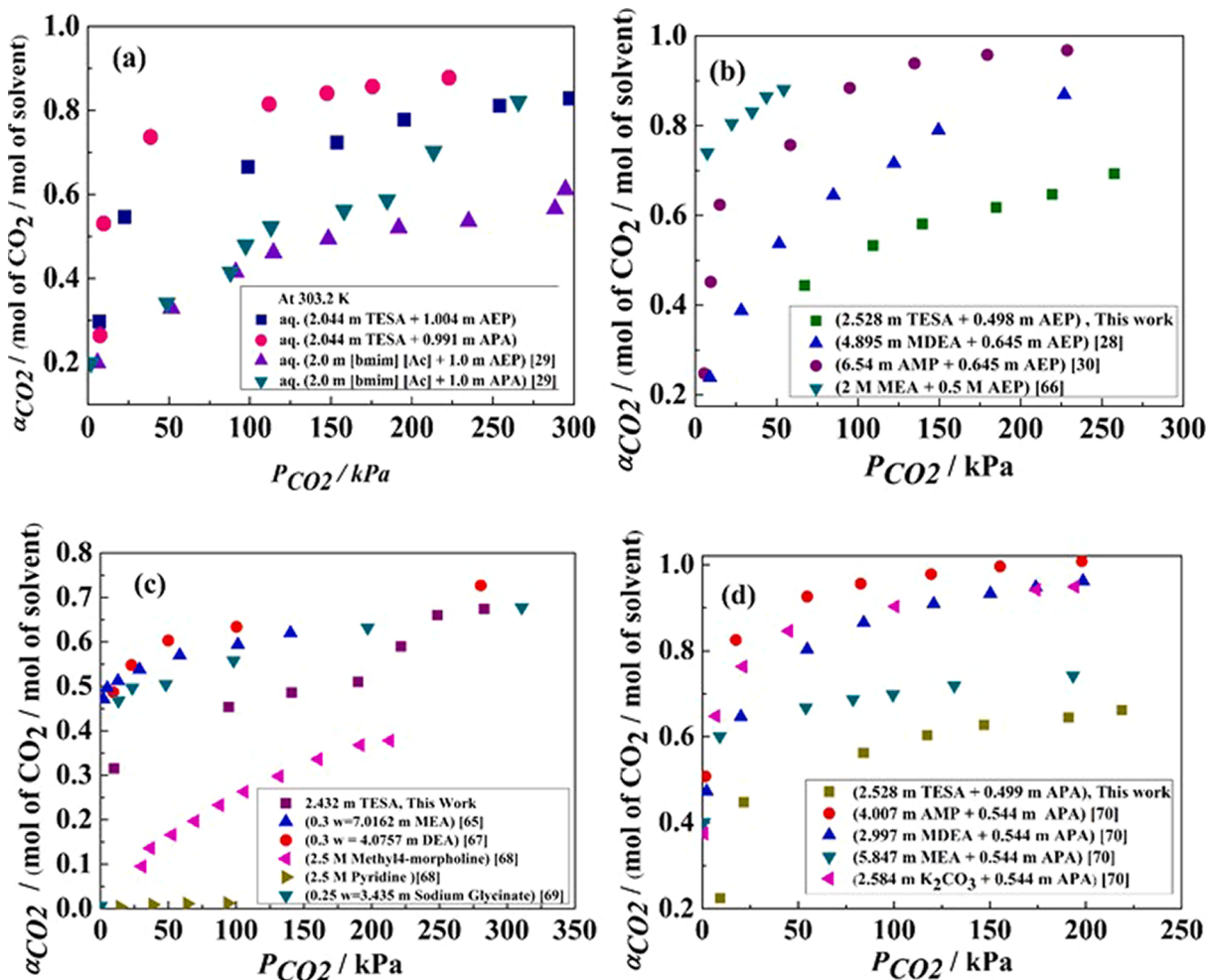


Fig. 10. Comparison of CO_2 solubility with literature (a) aq. (TESA + AEP/APA) at $T = 303.2\text{ K}$ (b) aq. (2.528 m TESA + 0.499 m APA) at 313.2 K (c) aq. (2.432 m TESA + 0.498 m AEP) at 313.2 K (‘m’ signifies ‘mol/kg’).

References

- [1] L.C. Ho, P. Babu, R. Kumar, P. Linga, HBGS (hydrate based gas separation) process for carbon dioxide capture employing an unstirred reactor with cyclopentane, *Energy* 63 (2013) 252–259.
- [2] Y. Huang, S. Rebennack, Q.P. Zheng, Techno-economic analysis and optimization models for carbon capture and storage: a survey, *Energy Syst.* 4 (2013) 315–353.
- [3] D.V. Marquez, A.F. Tlacuahuac, L.R. Sandoval, Techno-economic and dynamical analysis of a CO_2 capture pilot-scale plant using ionic liquids, *Ind. Eng. Chem. Res.* 54 (2015) 11360–11370.
- [4] A. Alhajaj, N.M. Dowell, N. Shah, A techno-economic analysis of post-combustion CO_2 capture and compression applied to a combined cycle gas turbine: part-II. Identifying the cost-optimal control and design variables, *Int. J. Greenh. Gas Con.* 52 (2016) 331–343.
- [5] D.H. Benito, J. Lemus, C. Moya, R. Santiago, V.R. Ferro, J. Palomar, Techno-economic feasibility of ionic liquids-based CO_2 chemical capture processes, *Chem. Eng. J.* 127196 (2020).
- [6] R. Carapellucci, L. Giordano, M. Vaccarelli, Application of an amine-based CO_2 capture system in retrofitting combined gas-steam power plants, *Energy* 118 (2017) 808–826.
- [7] M. Akbhari, P.V. Sheyda, CO_2 equilibrium solubility in and physical properties for monoethanolamine glycinate at low pressures, *Process Saf. Environ.* 132 (2019) 116–125.
- [8] S. Kumar, J.H. Cho, I. Moon, Ionic liquid-amine blends and CO_2 BOLs: Prospective solvents for natural gas sweetening and CO_2 capture technology- A review, *Int. J. Greenh. Gas Con.* 20 (2014) 87–116.
- [9] A. Ahmady, M.A. Hashim, M.K. Aroua, Absorption of carbon dioxide in the aqueous mixtures of methyldiethanolamine with three types of imidazolium based ionic liquids, *Fluid Phase Equilibr.* 309 (2011) 76–82.
- [10] V. Blasucci, R. Hart, V.L. Mestre, D.J. Hahne, M. Burlager, H. Huttenhower, B.J. R. Thio, P. Pollet, C.L. Liotta, C.A. Eckert, Single component, reversible ionic liquids for energy applications, *Fuel* 89 (2010) 1315–1319.
- [11] M.G. Miquel, M. Talreja, A.L. Ethier, K. Flack, J.R. Switzer, E.J. Biddinger, P. Pollet, J. Palomar, F. Rodriguez, C.A. Eckert, C.L. Liotta, COSMO-RS studies: structure-property relationships for CO_2 capture by reversible ionic liquids, *Ind. Eng. Chem. Res.* 51 (2012) 16066–16073.
- [12] A. Hemmati, R. Farahzad, A. Surendar, B. Aminahmadi, Validation of mass transfer and liquid holdup correlations for CO_2 absorption process with methyldiethanolamine solvent and piperazine as an activator, *Process Saf. Environ.* 126 (2019) 214–222.
- [13] Z.Z. Yang, Y.N. Zhao, L.N. He, CO_2 chemistry: task specific ionic liquids for CO_2 capture/activation and subsequent conversion, *RSC Adv.* 1 (2011) 545–567.
- [14] S. Lian, C. Song, Q. Liu, E. Duan, H. Ren, Y. Kitamura, Recent advances in ionic liquids-based hybrid processes for CO_2 capture and utilization, *J. Environ. Sci.* 99 (2021) 281–295.
- [15] M. Afkhamipour, M. Mofarahi, A. Rezaei, R. Mahmoodi, C.H. Lee, Experimental and theoretical investigation of equilibrium absorption performance of CO_2 using a mixed 1-dimethylamino-2-propanol (DMA2P) and monoethanolamine (MEA) solution, *Fuel* 256 (2019), 115877.
- [16] A. Schaffer, K. Brechtel, G. Scheffknecht, Comparative study on differently concentrated aqueous solutions of MEA and TETA for CO_2 capture from flue gases, *Fuel* 101 (2012) 148–153.
- [17] H. Zhou, X. Xu, X. Chen, G. Yu, Novel ionic liquids phase change solvents for CO_2 capture, *Int. J. Greenh. Gas Con.* 98 (2020), 103068.
- [18] M.S.R. Shahrom, C.D. Wilfred, A.K.Z. Taha, CO_2 capture by task specific ionic liquids (TSILs) and polymerized ionic liquids (PILs and AAPILs), *J. Mol. Liq.* 219 (2016) 306–312.
- [19] C.H. Huang, W. Klinthong, C.S. Tan, SBA-15 grafted with 3-aminopropyl triethoxysilane in supercritical propane for CO_2 capture, *J. Supercrit. Fluid* 77 (2013) 117–126.
- [20] W. Klinthong, C.H. Huang, C.S. Tan, CO_2 capture by mesoporous SBA-15 grafted with 3aminopropyl triethoxysilane in supercritical propane, *Energy Procedia* 37 (2013) 175–179.
- [21] M. Garip, N. Gizli, Ionic liquid containing amine-based silica aerogels for CO_2 capture by fixed bed adsorption, *J. Mol. Liq.* 310 (2020), 113227.
- [22] S.K. Dash, A.N. Samanta, S.S. Bandyopadhyay, Simulation and parametric study of post combustion CO_2 capture process using (AMP + PZ) blended solvent, *Int. J. Greenh. Gas Con.* 21 (2014) 130–139.

- [23] H. Li, Y.L. Moullec, J. Lu, J. Chen, J.C.V. Marcos, G. Chen, F. Chopin, CO₂ solubility measurement and thermodynamic modeling for 1-methylpiperazine/water/CO₂, *Fluid Phase Equilibr.* 394 (2015) 118–128.
- [24] Y. Yuan, B. Sherman, G.T. Rochelle, Effect of viscosity on CO₂ absorption in aqueous piperazine / 2-methylpiperazine, *Energy Procedia* 114 (2017) 2103–2120.
- [25] Y. Du, L. Li, O. Namjoshi, K.A. Voice, A.N. Fine, G.T. Rochelle, Aqueous piperazine / N-(2-aminoethyl) piperazine for CO₂ capture, *Energy Procedia* 37 (2013) 1621–1638.
- [26] S. Paul, A.K. Ghoshal, B.P. Mandal, Kinetics of absorption of carbon dioxide into aqueous solution of 2-(1-piperazinyl)-ethylamine, *Chem. Eng. Sci.* 64 (2009) 313–321.
- [27] S. Paul, A.K. Ghoshal, B.P. Mandal, Kinetics of absorption of carbon dioxide into aqueous blends of 2-(1-piperazinyl)-ethylamine and N-methyldiethanolamine, *Chem. Eng. Sci.* 64 (2009) 1618–1622.
- [28] A. Dey, S.K. Dash, B.P. Mandal, Equilibrium CO₂ solubility and thermophysical properties of aqueous blends of 1-(2-aminoethyl) piperazine and N-methyldiethanolamine, *Fluid Phase Equilibr.* 463 (2018) 91–105.
- [29] S. Balchandani, B.P. Mandal, S. Dharaskar, Measurements and modeling of vapor liquid equilibrium of CO₂ in amino activated imidazolium ionic liquid solvents, *Fluid Phase Equilibr.* 521 (2020), 112643.
- [30] A. Dey, S.K. Dash, S.C. Balchandani, B.P. Mandal, Investigation on the inclusion of 1-(2-aminoethyl) piperazine as a promoter on the equilibrium CO₂ solubility of aqueous 2-amino-2-methyl-1-propanol, *J. Mol. Liq.* 289 (2019), 111036.
- [31] B. Das, B. Deogam, B.P. Mandal, Experimental and theoretical studies on efficient carbon dioxide capture using novel bis (3-aminopropyl) amine (APA)-activated aqueous 2-amino-2-methyl-1-propanol (AMP) solutions, *RSC Adv.* 7 (2017) 21518–21530.
- [32] M. Mirarab, M. Sharifi, M.A. Ghayyem, F. Mirarab, Prediction of solubility of CO₂ in ethanol-[emim] [Tf₂N] ionic liquid mixtures using artificial neural networks based on genetic algorithm, *Fluid Phase Equilibr.* 371 (2014) 6–14.
- [33] A. Najafloo, A.T. Zoghi, F. Feyzi, Measuring solubility of carbon dioxide in aqueous blends of N-methyldiethanolamine and 2-(2-aminoethyl) amino ethanol at low CO₂ loadings and modelling by electrolyte SAFT-HR EoS, *J. Chem. Thermodynamics* 82 (2015) 143–155.
- [34] T. Sema, A. Naami, R. Idem, P. Tontiwachwuthikul, Correlations for equilibrium solubility of carbon dioxide in aqueous 4-(diethylamino)-2-butanol solution, *Ind. Eng. Chem. Res.* 50 (2011) 14008–14015.
- [35] A.K. Voice, S.J. Vavelstad, X. Chen, T. Nguyen, G.T. Rochelle, Aqueous 3-(methylamino) propylamine for CO₂ capture, *Int. J. Greenh. Gas Con.* 15 (2013) 70–77.
- [36] A.M. Pinto, H. Rodriguez, A. Ace, A. Soto, Carbon dioxide absorption in the ionic liquid 1-ethylpyridinium ethylsulphate and its mixture with another ionic liquid, *Int. J. Greenh. Gas Con.* 18 (2013) 296–304.
- [37] S.K. Dash, A. Samanta, A.N. Samanta, S.S. Bandyopadhyay, Vapour liquid equilibria of carbon dioxide in dilute and concentrated aqueous solutions of piperazine at low to high pressure, *Fluid Phase Equilibr.* 300 (2011) 145–154.
- [38] B.K. Mondal, S.S. Bandyopadhyay, A.N. Samanta, Vapor-liquid equilibrium measurement and ENRTL modeling of CO₂ absorption in aqueous hexamethylenediamine, *Fluid Phase Equilibr.* 402 (2015) 102–112.
- [39] P.F.D. Santos, L. Andre, M. Ducouso, F. Contamine, P. Cezac, Experimental measurement of CO₂ solubility in aqueous Na₂SO₄ solution at temperatures between 303.15 and 423.15 K and Pressures upto 20 MPa, *J. Chem. Eng. Data* 65 (2020) 3230–3239.
- [40] Y. Du, G.T. Rochelle, Thermodynamic modeling of aqueous piperazine / (N-(2-aminoethyl) piperazine for CO₂ capture, *Energy Procedia* 63 (2014) 997–1017.
- [41] C. A. Eckert, C. L. Liotta, Reversible Ionic Liquids as Double-Action Solvents for Efficient CO₂ Capture (technical report), Georgia Tech Research Corporation, Atlanta, 2011.
- [42] J.R. Switzer, A.L. Ethier, K.M. Flack, E.J. Biddinger, L. Gelbaum, P. Pollet, C. A. Eckert, C.L. Liotta, Reversible ionic liquid stabilized carbamic acids: a pathway toward enhanced CO₂ capture, *Ind. Eng. Chem. Res.* 52 (2013) 13159–13163.
- [43] C. Sun, P.K. Dutta, Infrared spectroscopic study of reaction of carbon dioxide with aqueous monoethanolamine solutions, *Ind. Eng. Chem. Res.* 55 (22) (2016) 6276–6283.
- [44] G. Richner, G. Puxty, Assessing the chemical speciation during CO₂ absorption by aqueous amines using in Situ FTIR, *Ind. Eng. Chem. Res.* 51 (2012) 14317–14324.
- [45] J. Choi, Y. Kim, S. Nam, S. Yun, Y. Yoon, J. Lee, CO₂ absorption characteristics of a piperazine derivative with primary, secondary, and tertiary amino groups, *Korean J. Chem. Eng.* 33 (2016) 3222–3230.
- [46] S.M. Hong, S.H. Kim, K.B. Lee, Adsorption of carbon dioxide on 3-aminopropyl-triethoxysilane modified graphite oxide, *Energy Fuels* 27 (6) (2013) 3358–3363.
- [47] D.V. Quang, T.A. Hatton, M.R.M.A. Zahra, Thermally stable amine-grafted adsorbent prepared by impregnating 3-aminopropyltriethoxysilane on mesoporous silica for CO₂ capture, *Ind. Eng. Chem. Res.* 55 (2016) 7842–7852.
- [48] L.F. Zubeir, G.E. Romanos, W.M.A. Wagelmans, B. Iliev, T.J.S. Schubert, M. Kroon, Solubility and diffusivity of CO₂ in the ionic liquid 1-butyl-3-methylimidazolium tricyanomethide within a large pressure range (0.01 MPa to 10 MPa), *J. Chem. Eng. Data* 60 (2015) 1544–1562.
- [49] A.T. Zoghi, A. Rahimi, F. Feyzi, A.H. Jalili, Measurement and modeling equilibrium solubility of carbon dioxide in aqueous solution of dimethylaminoethanol and 3-methylaminopropylamine, *Thermochim. Acta* 686 (2020), 178565.
- [50] M.E. Hamzehie, H. Najibi, Carbon dioxide loading capacity in aqueous solutions of potassium salt of proline blended with piperazine as new absorbents, *Thermochim. Acta* 639 (2016) 66–75.
- [51] B. Li, Y. Chen, Z. Yang, X. Ji, X. Lu, Thermodynamic study on carbon dioxide absorption in aqueous solutions of choline-based amino acid ionic liquids, *Sep. Purif. Technol.* 214 (2019) 128–138.
- [52] R. Haghbakhsh, H. Soleymani, S. Raeissi, A simple correlation to predict high pressure solubility of carbon dioxide in 27 commonly used ionic liquids, *J. Supercrit. Fluid* 77 (2013) 158–166.
- [53] R.L. Kent, B. Eisenberg, Better data for amine treating, *Hydrocarb. Process.* 55 (1976) 87–90.
- [54] Y.H. Hsu, R.B. Leron, M.H. Li, Solubility of carbon dioxide in aqueous mixtures of (reline + monoethanolamine) at T=(313.2 to 353.2) K, *J. Chem. Thermodyn.* 72 (2014) 94–99.
- [55] P.Y. Chung, A.N. Soriano, R.B. Leron, M.H. Li, Equilibrium solubility of carbon dioxide in the amine solvent system of (triethanolamine + piperazine + water), *J. Chem. Thermodyn.* 42 (2010) 802–807.
- [56] S. Shen, Y. Zhao, Y. Bian, Y. Wang, H. Guo, H. Li, CO₂ absorption using aqueous potassium lysinate solutions: vapor-liquid equilibrium data and modelling, *J. Chem. Thermodyn.* 115 (2017) 209–220.
- [57] M.N. Hassankiadeh, A. Jahangiri, Application of aqueous blends of AMP and piperazine to the low CO₂ partial pressure capturing: new experimental and theoretical analysis, *Energy* 165 (2018) 164–178.
- [58] M.J. Khodadadi, S. Riahi, M. Abbas, Experimental modeling of the solubility of carbon dioxide in aqueous solution of monoethanolamine + 1, 3-diaminopropane, *J. Mol. Liq.* 281 (2019) 415–422.
- [59] S. Kumar, R. Padhan, M.K. Mondal, Equilibrium solubility measurement and modeling of CO₂ absorption in aqueous blend of 2-(diethyl amino) ethanol and ethylenediamine, *J. Chem. Eng. Data* 65 (2020) 523–531.
- [60] J.S. Torrecilla, J. Palomar, J. Garcia, E. Rojo, F. Rodriguez, Modelling of carbon dioxide solubility in ionic liquids at sub and supercritical conditions by neural networks and mathematical regression, *Chemometr. Intell. Lab.* 93 (2008) 149–159.
- [61] F. Xu, H. Gao, H. Dong, Z. Wang, X. Zhang, B. Ren, S. Zhang, Solubility of CO₂ in aqueous mixtures of monoethanolamine and dicyanamide-based ionic liquids, *Fluid Phase Equilibr.* 365 (2014) 80–87.
- [62] G. Jing, L. Zhou, Z. Zhou, Characterization and kinetics of carbon dioxide absorption into aqueous tetramethylammonium glycinate solution, *Chem. Eng. J.* 181–182 (2012) 85–92.
- [63] Z. Feng, F.C. Gang, W.Y. Ting, W.Y. Tao, L.A. Min, Z.Z. Bing, Absorption of CO₂ in the aqueous solutions of functionalized ionic liquids and MDEA, *Chem. Eng. J.* 160 (2010) 691–697.
- [64] A.F. Portugal, P.W.J. Derkx, G.F. Versteeg, F.D. Magalhães, A. Mendes, Characterization of potassium glycinate for carbon dioxide absorption purposes, *Chem. Eng. Sci.* 62 (2007) 6534–6547.
- [65] K.P. Shen, M.H. Li, Solubility of carbon dioxide in aqueous mixtures of monoethanolamine with methylmethanolamine, *J. Chem. Eng. Data* 37 (1992) 96–100.
- [66] R. Ramazani, S. Mazinani, A. Hafizi, A. Jahanmiri, Equilibrium solubility of carbon dioxide in aqueous blend of monoethanolamine (MEA) and 2-1-piperazinyl-ethylamine (PZEA) solutions: experimental and optimization study, *Process Saf. Environ.* 98 (2015) 325–332.
- [67] D.J. Seo, W.H. Hong, Solubilities of carbon dioxide in aqueous mixtures of diethanolamine and 2-amino-2-methyl-1-propanol, *J. Chem. Eng. Data* 41 (1996) 258–260.
- [68] A. Nouacer, F.B. Belaribi, I. Mokbel, J. Jose, Solubility of carbon dioxide gas in some 2.5 M tertiary amine aqueous solutions, *J. Mol. Liq.* 190 (2014) 68–73.
- [69] B.K. Mondal, S.S. Bandyopadhyay, A.N. Samanta, VLE of CO₂ in aqueous sodium glycinate solution-new data and modeling using kent-eisenberg model, *Int. J. Greenh. Gas Con.* 36 (2015) 153–160.
- [70] B.K. Mondal, S.S. Bandyopadhyay, A.N. Samanta, Equilibrium solubility and enthalpy of CO₂ absorption in aqueous bis (3-aminopropyl) amine and its mixture with MEA, MDEA, AMP and K₂CO₃, *Chem. Eng. Sci.* 170 (2017) 58–67.